

This discussion paper is/has been under review for the journal Atmospheric Chemistry and Physics (ACP). Please refer to the corresponding final paper in ACP if available.

# Calibration of column-averaged CH<sub>4</sub> over European TCCON FTS sites with airborne in-situ measurements

M. C. Geibel<sup>1,\*</sup>, J. Messerschmidt<sup>2,\*\*</sup>, C. Gerbig<sup>1</sup>, T. Blumenstock<sup>3</sup>, F. Hase<sup>3</sup>, O. Kolle<sup>1</sup>, J. V. Lavrič<sup>1</sup>, J. Notholt<sup>2</sup>, M. Palm<sup>2</sup>, M. Rettinger<sup>4</sup>, M. Schmidt<sup>5</sup>, R. Süssmann<sup>4</sup>, T. Warneke<sup>2</sup>, and D. G. Feist<sup>1</sup>

<sup>1</sup>Max Planck Institute for Biogeochemistry (MPI-BGC), Jena, Germany

<sup>2</sup>Institute of Environmental Physics (IUP), University of Bremen, Bremen, Germany

<sup>3</sup>IMK-ASF, Karlsruhe Institute of Technology (KIT), Karlsruhe, Germany

<sup>4</sup>IMK-IFU, Karlsruhe Institute of Technology (KIT), Garmisch-Partenkirchen, Germany

<sup>5</sup>Laboratoire des Sciences du Climat et l'Environnement (LSCE), Gif-sur-Yvette, France

\* now at: Department for Applied Environmental Research (ITM), Stockholm University, Stockholm, Sweden

\*\* now at: California Institute of Technology, Pasadena, CA, USA

Received: 22 December 2011 – Accepted: 7 January 2012 – Published: 17 January 2012

Correspondence to: D. G. Feist (dfeist@bge-jena.mpg.de)

Published by Copernicus Publications on behalf of the European Geosciences Union.

ACPD

12, 1517–1551, 2012

Discussion Paper | Discussion Paper

Calibration of column-averaged CH<sub>4</sub> over European TCCON sites

M. C. Geibel et al.

Title Page

Abstract

Introduction

Conclusions

References

Tables

Figures

◀

▶

Back

Close

Full Screen / Esc

Printer-friendly Version

Interactive Discussion



## Abstract

In September/October 2009, six ground-based Fourier Transform Spectrometers (FTS) of the Total Carbon Column Observation Network (TCCON) in Europe were calibrated with aircraft in-situ measurements for the first time. The campaign was part of the

5 Infrastructure for Measurement of the European Carbon Cycle (IMECC) project.

During this campaign aircraft in-situ profiles of CO<sub>2</sub>, CH<sub>4</sub>, CO and H<sub>2</sub>O (from continuous measurements) as well as N<sub>2</sub>O, H<sub>2</sub>, and SF<sub>6</sub> (from flasks) were taken close to the FTS sites. The aircraft data had a vertical coverage ranging from approximately 300 to 13 000 m, corresponding to ~80 % of the total atmospheric column seen by the

10 FTS.

This study summarizes the calibration results for CH<sub>4</sub>. Using similar methods, the resulting calibration factor of  $0.978 \pm 0.002$  ( $\pm 1\sigma$ ) from the IMECC campaign agreed very well with the results that Wunch et al. (2010) had derived for TCCON instruments in North America, Australia, New Zealand, and Japan. By adding the data of the previous calibration of Wunch et al. (2010), the uncertainty of the calibration factor could be reduced by a factor of three.

A careful analysis of the calibration method used by Wunch et al. (2010) revealed that the incomplete vertical coverage of the aircraft profiles can lead to a bias in the calibration factor. This bias can be compensated with a new iterative approach that we developed. Using this improved method, we derived a significantly lower calibration factor of  $0.974 \pm 0.002$  ( $\pm 1\sigma$ ). This corresponds to a correction of all TCCON CH<sub>4</sub> measurements by roughly -7 ppb.

## 1 Introduction

The Total Carbon Column Observation Network (TCCON) is a worldwide network 25 of ground-based Fourier Transform Spectrometers (FTS). It currently consists of 18 sites that provide a source for calibration and validation of satellite measurements like

[Title Page](#)

[Abstract](#)

[Introduction](#)

[Conclusions](#)

[References](#)

[Tables](#)

[Figures](#)

◀

▶

[Back](#)

[Close](#)

[Full Screen / Esc](#)

[Printer-friendly Version](#)

[Interactive Discussion](#)



GOSAT (Yokota et al., 2009; Morino et al., 2010) and the upcoming OCO-2 (Crisp et al., 2004). Unlike surface measurements, the FTS data can be used directly for the validation since the data product (total column abundances) is similar.

TCCON also complements the in-situ measurement network by delivering column integrals of different species (e.g. CO<sub>2</sub>, CH<sub>4</sub>) in the form of volume mixing ratios (VMR) (Wunch et al., 2011). In contrast to the ground-based in-situ network, total column measurements are not limited to the atmospheric boundary layer and are thus less sensitive to local sources and sinks and details of vertical transport (Gerbig et al., 2008). However, the reduced sensitivity of total column measurements to local influences makes the identification of seasonal and latitudinal variations of CO<sub>2</sub> and CH<sub>4</sub> challenging.

The integration of the TCCON FTS measurements into the existing ground-based in-situ network requires a calibration. Different measurement techniques do not necessarily produce equal measurement values – even when they are measuring exactly the same physical quantity. Besides that, it is important to investigate possible biases within TCCON that might lead to major errors in the source/sink estimation of inverse modelling (Rayner and O'Brien, 2001). Wunch et al. (2010) showed that there is a species-specific uniform calibration factor for the calibrated FTS systems and assumes that the cause for differences between in-situ and FTS measurements is based in uncertainties of the spectroscopic line list that is used for the FTS data retrieval. Thus, it is highly likely that those species-specific uniform calibration factors apply for all FTS instruments of TCCON.

This article discusses the results of the CH<sub>4</sub> calibration. In a second step, it investigates improvements of the calibration method used by Wunch et al. (2010).

## 2 The IMECC campaign

The first airborne campaign to calibrate FTS sites in Europe was part of the Infrastructure for Measurement of the European Carbon Cycle (IMECC), an Integrated

## Calibration of column-averaged CH<sub>4</sub> over European TCCON sites

M. C. Geibel et al.

[Title Page](#)

[Abstract](#)

[Introduction](#)

[Conclusions](#)

[References](#)

[Tables](#)

[Figures](#)

◀

▶

◀

▶

[Back](#)

[Close](#)

[Full Screen / Esc](#)

[Printer-friendly Version](#)

[Interactive Discussion](#)



**Calibration of column-averaged CH<sub>4</sub> over European TCCON sites**

M. C. Geibel et al.

[Title Page](#)[Abstract](#)[Introduction](#)[Conclusions](#)[References](#)[Tables](#)[Figures](#)[◀](#)[▶](#)[◀](#)[▶](#)[Back](#)[Close](#)[Full Screen / Esc](#)[Printer-friendly Version](#)[Interactive Discussion](#)

Infrastructure Initiative within the European Union's 6th Framework Programme. Its main purpose was the calibration of five European TCCON sites and one mobile TCCON instrument (Geibel et al., 2010).

Two European TCCON FTS sites (OR and BI) were co-located with tall tower stations. Figure 1 shows the five European TCCON sites, the mobile FTS in Jena, Germany, the airbase in Hohn, Germany, and the flight tracks of the IMECC campaign. Three other European TCCON sites (Sodankylä, Izana, Ny-Ålesund) could not be reached by the aircraft during this campaign.

The campaign took place between 28 September and 9 October 2009. The aircraft used was a Learjet 35A, operated by Enviscope/GfD. The in-situ profiles were taken near the FTS sites in the form of spirals from the maximum flight altitude of ~13 000 m down to ~300 m (see Figs. 2 and 3). Additional dips were made during the transfer flights. Overall eight flights in four days were realized. In about 20 flight hours 16 vertical profiles over the European TCCON sites were sampled at different solar zenith angles (SZA). The details of the overflights are listed in Table 1.

During the campaign, the FTS sites were operated by the individual working groups that are responsible for each site. Three sites are operated by the Institute of Environmental Physics (IUP), Bremen, Germany; one site by IMK-ASF, Karlsruhe Institute of Technology (KIT), Karlsruhe, Germany; one by IMK-IFU (KIT), Garmisch-Partenkirchen, Germany; and one by the Max Planck Institute for Biogeochemistry (MPI-BGC), Jena, Germany. The FTS instruments at these sites were Bruker IFS 125 HR spectrometers and were equipped according to TCCON standards. Only the Karlsruhe FTS covered the mid-infrared region with a liquid-N<sub>2</sub>-cooled InSb detector and therefore had a limited bandwidth for the Indium Gallium Arsenide (InGaAs) detector. The instrumental settings used during the campaign and a detailed description of the different sites can be found in Messerschmidt et al. (2011).

During the whole campaign in-situ data of CO<sub>2</sub>, CH<sub>4</sub>, H<sub>2</sub>O and CO were taken on board the aircraft. In addition to the in-situ data, up to eight flasks were taken at different altitude levels per profile. These flasks were analyzed for CO<sub>2</sub> and its isotopes,

CH<sub>4</sub>, N<sub>2</sub>O, CO, H<sub>2</sub> and SF<sub>6</sub>. The results were used to assure the quality of the continuous measurements. The flasks were analyzed post-flight at the gas analysis lab of the Max Planck Institute for Biogeochemistry, Jena. Supplemental meteorological (air temperature, pressure and relative humidity) data were recorded. The overall distance flown during the IMECC campaign was approximately 12 000 km.

Detailed information about the aircraft instrumentation and in-situ data can be found in Messerschmidt et al. (2011).

### 3 FTS data processing

To ensure a uniform processing of the FTS data obtained within the IMECC campaign,

all spectra of the participating sites were processed in Jena using identical software and settings for all sites. For the analysis of the spectral data the TCCON standard retrieval software GFIT (Wunch et al., 2011) was used with the same settings as used in Wunch et al. (2010).

The uncertainties of the GFIT retrieval are a combination of statistical errors (residuals from the spectral fits) and systematic artifacts (e.g. errors/omissions in the spectroscopy, the modeling of the instrument response, and pointing-induced solar line shifts) (Wunch et al., 2011). The uncertainty estimation – the GFIT error – is a standard product of the GFIT software.

#### FTS data pre-processing for correction of solar intensity variations

The weather situation during the IMECC campaign was not optimal for FTS measurements. Although the flights were scheduled using forecast products and satellite imagery, many sites suffered from cloudy sky conditions during the overflights. This introduces solar intensity variations (SIV) to the measured interferograms. To enhance the quality of the spectra for further analysis, all FTS spectra of all participating sites were pre-processed with the Interferogram Processing Program (IPP).

## Calibration of column-averaged CH<sub>4</sub> over European TCCON sites

M. C. Geibel et al.

[Title Page](#)

[Abstract](#)

[Introduction](#)

[Conclusions](#)

[References](#)

[Tables](#)

[Figures](#)

◀

▶

◀

▶

[Back](#)

[Close](#)

[Full Screen / Esc](#)

[Printer-friendly Version](#)

[Interactive Discussion](#)



# Calibration of column-averaged $\text{CH}_4$ over European TCCON sites

M. C. Geibel et al.

The method of correction of SIVs was described by Keppel-Aleks et al. (2007). It is based on the idea that division of the interferogram by the unmodulated DC detector signal restores the interferogram fringes to their correct amplitudes. An example of the effect that this has on the spectrum can be seen in Fig. 4. The signal to noise (S/N) ratio increases significantly, the absorption lines are sharper and therefore easier to retrieve.

Keppel-Aleks et al. (2007) implemented this scheme into the IPP software and applied this method to Park Falls and Darwin TCCON data. They showed that on partly cloudy days the pre-processing of the spectral data with the IPP software substantially reduces the scatter of the results of the GFIT retrieval. The same effect could be reproduced with the data of the IMECC campaign and is shown here for the example of Bialystok (see Fig. 5).

The scatter was reduced significantly: from a standard deviation of 4.2 ppb without SIV correction to 1.3 ppb with SIV correction. Also the “early morning feature” around 06:00 UTC, which was probably caused by cloud affected spectra, could be corrected. The error bars of the early morning measurements were reduced: the ratio of mean error with SIV correction to mean error without SIV correction was 0.68 for spectra obtained before 06:30 UTC. Some outliers that were out of the plotting range could be better retrieved (some however with large error bars).

20 In general, the data pre-processing with the IPP software was able to increase the quality of the spectral data used for the calibration process.

## 4 Data analysis

25 Data analysis was performed separately for CO<sub>2</sub> and CH<sub>4</sub>. This section describes  
the results of the CH<sub>4</sub> calibration. The results of the CO<sub>2</sub> calibration can be found in  
Messerschmidt et al. (2011).

Title Page

## Abstract

Introduction

## Conclusions

## References

## Tables

## Figures

1

▶

1

▶

Back

Close

Full Screen / Esc

[Printer-friendly Version](#)

## Interactive Discussion



## 4.1 Method of intercomparison of two different measurement principles

As pointed out in Sect. 1, in-situ and FTS data can not be compared directly. Airborne in-situ data deliver information of abundances of one or more species in the form of a profile (see Sect. 2). This profile has a high vertical resolution, however, the vertical coverage is limited to less than 80 % of the total column. The aircraft data can only deliver a partial column. For the calibration, the aircraft profile has to be extended to an artificial aircraft total column (see Sect. 4.3).

FTS spectral data deliver total column dry air mole fractions (DMF) for the individual species. The vertical coverage of this type of measurement can be seen as unlimited, since it covers all parts of the atmosphere from the radiation source (sun) to the spectrometer (surface). The results of the GFIT retrieval deliver no information of the vertical distribution of the species. Rodgers and Connor (2003) developed a method that allows the intercomparison of two different measurement methods where one has a much higher resolution than the other. This method is adapted for the intercomparison of aircraft and FTS data after vertical integration:

$$\widehat{c}_s = \gamma c_a + \mathbf{A}^T (\mathbf{x}_h - \gamma \mathbf{x}_a) \quad (1)$$

with  $\widehat{c}_s$ : retrieved DMF based on airborne measurements,  $\gamma$ : FTS retrieval scaling factor,  $c_a$ : FTS a-priori DMF,  $\mathbf{A}$ : FTS column averaging kernel,  $\mathbf{x}_h$ : aircraft profile (extended),  $\mathbf{x}_a$ : FTS a-priori profile. Please note that  $\gamma$  is an internal variable of the GFIT retrieval and not the calibration factor that was mentioned in Sect. 1.

As pointed out by Wunch et al. (2010), for a GFIT scaling retrieval the averaging kernels are calculated for the scaled solution mole fraction profile. Thus the linearization point of the Taylor expansion producing Eq. (1) is  $\gamma \mathbf{x}_a$  and not  $\mathbf{x}_a$ .

Wunch et al. (2010) used the method of Rodgers and Connor (2003) for the analysis of earlier calibration campaigns. The derivation of the equation of the column-averaged aircraft CH<sub>4</sub> DMF can be found in Wunch et al. (2010):

[Title Page](#)[Abstract](#)[Introduction](#)[Conclusions](#)[References](#)[Tables](#)[Figures](#)[◀](#)[▶](#)[Back](#)[Close](#)[Full Screen / Esc](#)[Printer-friendly Version](#)[Interactive Discussion](#)

$$\widehat{c}_s = \gamma \frac{\Gamma_{\text{CH}_4}^{\text{apriori}}}{\Gamma_{\text{dry air}}} + \left( \frac{\Gamma_{\text{CH}_4, \text{ak}}^{\text{aircraft}} - \gamma \Gamma_{\text{CH}_4, \text{ak}}^{\text{apriori}}}{\Gamma_{\text{dry air}}} \right) \quad (2)$$

with  $\gamma$ : FTS retrieval scaling factor,  $\Gamma_{\text{dry air}}$ : total column of dry air,  $\Gamma_{\text{CH}_4}^{\text{apriori}}$ : total vertical column of  $\text{CH}_4$ ,  $\Gamma_{\text{CH}_4, \text{ak}}^{\text{aircraft}}$ : column averaging kernel-weighted vertical column of the aircraft,  $\Gamma_{\text{CH}_4, \text{ak}}^{\text{apriori}}$ : column averaging kernel-weighted vertical a-priori.

5 The presented method uses the aircraft profile extended to a total column, the FTS dry air mole fractions, the GFIT a-priori profiles, the retrieval scaling factor, and the GFIT averaging kernels (AK) to retrieve the DMF of the extended aircraft column. This result is then used to calculate the calibration factor for the FTS measurements (see Sect. 5.1).

10 The GFIT a-priori profiles are based on MkIV balloon profiles and profiles obtained from the Atmospheric Chemistry Experiment (ACE-FTS) on-board SCISAT-1 – both measured in the 30–40° N latitude range from 2003 to 2007. With the help of auxiliary data specific to the location and time of the FTS measurement (air temperature (AT),

15 geopotential height (GH), specific humidity (SH), and tropopause pressure (TP) from the NCEP database, Kalnay et al., 1996) they are converted to a local a-priori profile for each day. Within the GFIT analysis this local a-priori profile is weighted with an SZA-dependent averaging kernel and scaled with a retrieval scaling factor to perform a spectral fit of the measured spectral data.

## 4.2 Correction of GFIT a-priori $\text{CH}_4$ profiles via HF correlation

20 As indicated by Wunch et al. (2010) for a more precise retrieval of  $X_{\text{CH}_4}$  the estimated tropopause heights of the GFIT a-priori  $\text{CH}_4$  profiles have to be corrected. This is done by using the correlation of methane and hydrofluoric acid (HF) that was observed by Luo et al. (1995) and Washenfelder et al. (2003). The  $\text{CH}_4$ -HF-correlation is based on

## Calibration of column-averaged $\text{CH}_4$ over European TCCON sites

M. C. Geibel et al.

[Title Page](#)

[Abstract](#)

[Introduction](#)

[Conclusions](#)

[References](#)

[Tables](#)

[Figures](#)

◀

▶

◀

▶

[Back](#)

[Close](#)

[Full Screen / Esc](#)

[Printer-friendly Version](#)

[Interactive Discussion](#)



## Calibration of column-averaged CH<sub>4</sub> over European TCCON sites

M. C. Geibel et al.

[Title Page](#)

[Abstract](#)

[Introduction](#)

[Conclusions](#)

[References](#)

[Tables](#)

[Figures](#)

◀

▶

[Back](#)

[Close](#)

[Full Screen / Esc](#)

[Printer-friendly Version](#)

[Interactive Discussion](#)



the complete absence of HF in the troposphere.

To apply this correction the results of a GFIT X<sub>HF</sub> retrieval for the individual site are used to calculate an altitude shift for the CH<sub>4</sub> a-priori profiles (see Fig. 6). The modified GFIT a-priori profiles were used for a re-analysis of all IMECC spectral data.

### 4.3 Aircraft total column extension

The FTS measurements cover the whole atmosphere, from the surface to the top of the stratosphere. Airborne in-situ measurements, like those performed during the IMECC campaign, have limited vertical coverage. It is impossible to measure at the surface due to the lack of an airport close to the FTS sites, or to reach altitudes higher than ~13 km to cover the upper part of the atmosphere. In most cases the aircraft data are limited to an altitude range from approximately 300 to 13 000 m. Thus the aircraft can only deliver a partial column. To compare the aircraft data with the FTS data, this partial column has to be extended to a total column.

For the FTS sites Orleans and Bialystok, ground-based in-situ data from the co-located tall-tower stations Trainou (TRN) and Bialystok (BIK), respectively, were used to extend the aircraft data to the ground. For the other sites the values measured at the lowermost altitude by the aircraft were linearly extrapolated to the surface. The uncertainty was estimated conservatively using the variance of the lowest aircraft data. For the stratospheric part of the column the GFIT a-priori profile weighted with the retrieval scaling factor was used (see Fig. 7). The a-priori profile was then weighted with the GFIT averaging kernel and scaled by the retrieval scaling factor for the individual overflight (see Sect. 4.1). The error of the stratospheric mixing ratio was estimated conservatively as 1 % of the scaled and weighted a-priori. This corresponds to the shifting of the profile by 1 km up and down performed by Wunch et al. (2010). An overview of the individual uncertainties of the extrapolation to the ground, the stratospheric extension by using the GFIT a-priori and the aircraft data can be found in Table 2. The extended aircraft columns were then used to calculate the aircraft DMF needed for Eq. (1).

In-situ measurements and FTIR measurements rely on different basic principles. The in-situ measurements are ultimately based on the fundamental constants and standards used in mass spectroscopy while the FTIR measurements rely on spectroscopic parameters like line strength from spectral line catalogs. Even under ideal conditions measurements of the same airmass with both methods would not produce exactly the same result. For example, even the slightest deviation in the strength of a spectral line would produce a scaling offset from the in-situ result. This fundamental difference is acknowledged by introducing a calibration factor  $\psi$  between the two methods. This calibration factor is expected to be close to but not exactly one. In principle, this calibration factor may consist of a method-dependent part (for example spectroscopic data) and an instrument-dependent part.

For the derivation of the calibration factor obviously a data point consisting of an aircraft value and an FTS value for each overflight is needed. The aircraft value was calculated by integrating the extended aircraft column. All spectral data within a time window of  $\pm 30$  min around the spectrum closest to the aircraft overflight were chosen. As a data quality criterion all spectra with a GFIT error larger than 10 ppb were excluded (see Sect. 3). For spectra fulfilling both criteria the median value of the DMF was calculated. This value represents the FTS data point for calibration.

In a first step, the results of the GFIT retrievals with standard a-priori profiles were investigated. Similar to Wunch et al. (2010) the data points were fitted with an error-weighted least-squares fit as published in York et al. (2004) to derive the calibration factor  $\psi_{\text{std}}$ . In agreement with the previous investigation of Wunch et al. (2010), an artificial calibration point at the origin was added (D. Wunch, personal communication, 2010).

The fit of the IMECC campaign data produces a calibration factor of  $\psi_{\text{std}} = 0.978 \pm 0.002$  ( $\pm 1\sigma$ ). Although derived with GFIT standard a-priori profiles, it is already similar

## Calibration of column-averaged $\text{CH}_4$ over European TCCON sites

M. C. Geibel et al.

Title Page

## Abstract

Introduction

## Conclusions

## References

Tables

## Figures



Back

Close

Full Screen / Esc

Printer-friendly Version

## Interactive Discussion



**Calibration of column-averaged CH<sub>4</sub> over European TCCON sites**

M. C. Geibel et al.

[Title Page](#)[Abstract](#)[Introduction](#)[Conclusions](#)[References](#)[Tables](#)[Figures](#)[◀](#)[▶](#)[◀](#)[▶](#)[Back](#)[Close](#)[Full Screen / Esc](#)[Printer-friendly Version](#)[Interactive Discussion](#)

to the results of the earlier campaign (Wunch et al., 2010). To be able to compare the results of the IMECC campaign data with the data of Wunch et al. (2010), however, the GFIT retrieval had to be repeated using the extended aircraft profile from Sect. 4.3 as the a-priori profile for the GFIT retrieval. The different a-priori has minor effects of ±2 ppb on the retrieval for the individual sites. This is on the same order of magnitude as the typical GFIT error for CH<sub>4</sub>. Figure 8 shows the results of the fit for this procedure (continuous line). The resulting calibration factor  $\psi_{\text{aircraft}} = 0.978 \pm 0.002$  is exactly the same as  $\psi_{\text{std}}$  and the one derived by Wunch et al. (2010).

In the next step, the Wunch et al. (2010) data were added to the dataset and the fitting procedure was repeated (see dashed line in Fig. 8) to derive a calibration factor  $\psi_{I+W}$  for all sites (IMECC + Wunch et al.). As a result, the calibration factor does not change, but the uncertainty is reduced by ∼68 % (from ±0.00205 to ±0.00066).

To illustrate the quality of the fit, the residuals ( $\text{DMF}_{\text{FTS}} - \psi_{I+W} \text{DMF}_{\text{aircraft}}$ ) for all calibration points are shown in Fig. 9. For overflights with a larger error bar, the residuals indicate a tendency to a slightly higher calibration factor than the one derived by Wunch et al. (2010). However, most of the calibration points include the calibration factor with their error bars and have their median well within the same range as the data from Wunch et al. (2010) (±10 ppb).

## 5.2 Influence of the individual overflights of the IMECC sites on the calibration factor

To test the hypothesis that an independent calibration factor is needed for each FTS site, each overflight was analyzed separately. The York et al. (2004) fitting procedure was used to derive a separate calibration factor for each individual overflight and one based on all other overflights. Figure 10 shows an overlap of the error bars with the calibration factor for 11 of 16 overflights. This corresponds to 68.8 % and confirms expectations for ±1- $\sigma$  error bars.

## 5.3 Influence of the amount of aircraft data on the calibration points

An important factor for the calculation of the calibration factor is the vertical coverage of aircraft data in the artificial aircraft total column as shown in Sect. 4.3. The less aircraft information available, the more the a-priori has to be used to fill the profile.

- 5 To illustrate the effect of the vertical coverage of aircraft data in the aircraft total column, a sensitivity test was performed. The vertical coverage of aircraft data was artificially reduced to data measured below a certain pressure value. The remaining part of the column was filled with the scaled and AK-weighted a-priori (see Sect. 4.3). Then the calibration point (FTS-to-aircraft ratio) was re-calculated. The results show  
10 the expected behavior of an increasing FTS-to-aircraft ratio with the decrease of the vertical coverage of aircraft data (see Fig. 11a).

In an extreme scenario of no aircraft data, the profile is identical with the scaled a-priori. For Eq. (1) in Sect. 4.1 the consequences are that the calibration factor becomes 1. With fewer aircraft measurements, one is left to rely more upon a-priori knowledge about the calibration factor. In the case of no aircraft data this means no information about the calibration factor.  
15

Having these results in mind when looking at the individual aircraft profiles in Sect. 4.3, it is obvious that one can expect different behavior of different overflights due to the vertical coverage of aircraft data.

- 20 A good example are the first two overflights over Jena. Overflight JE-OF1a has a maximum flight altitude of 13 km, overflight JE-OF1b of approximately 8 km. Due to the time difference between overflight and first spectrum, for these calibration points exactly the same FTS data are used. The aircraft data are similar as well. Hence, the difference in the residuals in Fig. 9 for these two calibration points is most likely  
25 due to the different amount of aircraft data. The residual of JE-OF1a is smaller and the calibration factor for this individual calibration point closer to 0.978. The residual of JE-OF1b, however, is larger and the calibration factor for this individual calibration point further away from 0.978 (see Fig. 10).

## 6 An improved approach to determine the calibration factor

The previous results have shown that the calibration points with aircraft profiles with less vertical coverage are biased towards 1. This is caused by the extrapolation of the aircraft profiles with the GFIT a-priori. The less aircraft information contributes to the 5 extended aircraft total column, the more the extended aircraft column tends towards the GFIT a-priori.

A simplified example can illustrate the problem. Figure 12 shows two measurements on an artificial pressure level. Measurement A represents the scaled FTS a-priori profile (which, if integrated, is equal to the FTS DMF) and covers the complete pressure 10 range (total column). Measurement B represents the aircraft profile and covers the lower 50 % of the pressure range (partial column). Measurements A and B are constant ( $A = 1$ ,  $B = 3$ ). The true calibration factor is known in this example ( $\psi_{\text{true}} = 1/3$ ).

Following the procedure of Wunch et al. (2010), measurement B is extrapolated to the full total column by using measurement A. This leads to an integrated profile for B 15 and a calibration factor that is biased towards 1 ( $\psi_{\text{int}} = 1/2$ ).

This shows, that the extrapolation of the aircraft profile with the FTS a-priori generally leads to a bias of the calibration factor towards 1. The magnitude of this bias depends on the amount of aircraft data and the difference of the calibration factor from 1.

A possible solution for this problem is to extrapolate measurement B with a 20 calibration-factor-corrected measurement A to derive the true calibration factor. To be able to do this, the calibration factor has then to be derived in an iterative calculation.

Following this principle, the aircraft column has to be extrapolated with a calibration-factor-corrected GFIT a-priori profile (see Fig. 13). The approach of Rodgers and Connor (2003) (see Eq. 1) is modified to:

$$25 \quad \widehat{c}_s = \frac{\gamma c_a}{\psi_n} + \mathbf{A}^T \left( \mathbf{x}_h - \frac{\gamma \mathbf{x}_a}{\psi_n} \right) \quad (3)$$

with  $\widehat{c}_s$ : retrieved DMF of the aircraft,  $\gamma$ : FTS retrieval scaling factor,  $c_a$ : FTS a-priori DMF,  $\mathbf{A}$ : FTS column averaging kernel,  $\mathbf{x}_h$ : aircraft profile,  $\mathbf{x}_a$ : FTS a-priori profile,  $\psi_n$ :

[Title Page](#)

[Abstract](#)

[Introduction](#)

[Conclusions](#)

[References](#)

[Tables](#)

[Figures](#)

[◀](#)

[▶](#)

[Back](#)

[Close](#)

[Full Screen / Esc](#)

[Printer-friendly Version](#)

[Interactive Discussion](#)



## Calibration of column-averaged CH<sub>4</sub> over European TCCON sites

M. C. Geibel et al.

[Title Page](#)

[Abstract](#)

[Introduction](#)

[Conclusions](#)

[References](#)

[Tables](#)

[Figures](#)

◀

▶

◀

▶

[Back](#)

[Close](#)

[Full Screen / Esc](#)

[Printer-friendly Version](#)

[Interactive Discussion](#)



iteratively-derived calibration factor.

Starting from a calibration factor  $\psi_0 = 1$ , the calibration points are calculated and the fitting procedure (see Sect. 5.1) is applied. This leads to a new calibration factor  $\psi_1$ . The procedure is repeated until the factor converges to the final value  $\psi_n$ . Since the a-priori profile only has a small influence on the GFIT retrieval (see Sect. 5.1), the GFIT retrieval with a  $\psi_n$ -corrected aircraft profile as a-priori for each iteration step was not performed for this study. The new extended aircraft profiles (see Fig. 13) show that the aircraft profiles extrapolated with the iteratively scaled a-priori are no longer affected by a bias towards 1. Profiles with less aircraft information are now closer to the calibration-factor-scaled a-priori profile.

To illustrate the effect of the iterative approach, the analysis of Sect. 5.3 was repeated. The results can be seen in Fig. 11b.

In contrast to the method used by Wunch et al. (2010) (see Fig. 11a), an artificial limitation of the amount of aircraft data no longer leads to a convergence of the calibration factor towards 1. Using the iterative approach, overflights with less aircraft data cause no bias in the calibration factor.

The resulting calibration factor for the IMECC campaign dataset  $\psi_n = 0.974 \pm 0.002$  ( $\pm 1\sigma$ ) (see Fig. 14, upper part) is significantly different from the one derived by the method of Wunch et al. (2010).

By using this iterative approach, the calibration points of the individual overflights show roughly the same scatter and residuals (see Fig 14, lower part) as in the approach of Wunch et al. (2010) (see Figs. 8 and 9). The standard deviation for both residual calculations is the same (6 ppb). Temporally close overflights (BI-OF2a/b, OR-OF1a/b) with different maximum flight altitudes, however, are now more consistent. The influence of the vertical coverage of the aircraft data is reduced to a minimum. The difference of 0.004 between  $\psi_{l+w}$  and  $\psi_n$  corresponds to a ~7 ppb offset for the FTS DMFs.

## 7 Conclusions

Using the same method as Wunch et al. (2010), the results of the IMECC aircraft campaign confirmed the earlier calibration factor for  $\text{CH}_4$ . When the results of Wunch et al. (2010) and the IMECC campaign were combined, the uncertainty of the fit of the calibration factor could be reduced by  $\sim 68\%$  (see Table 3). It seems to be most likely that this factor is a uniform calibration factor for the whole TCCON network.

However, further investigation of the method of Wunch et al. (2010) shows that stratospheric extrapolation of the aircraft data is sensitive to the vertical coverage of the aircraft data and introduces a bias of the calibration factor. An uniform vertical coverage of the aircraft data is, unfortunately, not always possible. Besides that, the uncertainties of the stratospheric part lead to significant uncertainties for the aircraft DMF and generate  $\sim 85\%$  of the total error budget. A better knowledge about the stratospheric distribution of  $\text{CH}_4$  is needed to be able to reduce these errors and thus improve the calibration procedure.

An iterative determination of the calibration factor presents a possible solution for the problem of different vertical coverage of the aircraft data and removes the bias resulting from the stratospheric extrapolation. The improved iterative method produced a slightly smaller calibration factor than the method of Wunch et al. (2010). For typical atmospheric values of  $\text{CH}_4$  DMF this corresponds to a high-bias of about +7 ppb in the published Wunch et al. (2010)  $\text{CH}_4$  data. This value corresponds to roughly twice the typical GFIT error for  $\text{CH}_4$ . Further investigations with more calibration points (e.g. IMECC + data from Wunch et al., 2010) have to validate the results of this approach.

Apart from the iterative method, there are two options to avoid this problem:

- The retrieval of a partial column from FTS spectral data that has the same vertical coverage as the aircraft profile. This method is not currently possible since the GFIT software for the retrieval of FTS DMFs does not yet allow partial column retrieval. Besides that, this would not allow a calibration of the TCCON standard

## Calibration of column-averaged $\text{CH}_4$ over European TCCON sites

M. C. Geibel et al.

[Title Page](#)

[Abstract](#)

[Introduction](#)

[Conclusions](#)

[References](#)

[Tables](#)

[Figures](#)



[Back](#)

[Close](#)

[Full Screen / Esc](#)

[Printer-friendly Version](#)

[Interactive Discussion](#)



product (total column DMFs) and partial column retrievals pose the risk of higher uncertainties than those for total column retrieval.

- 5 – Future calibration campaigns with balloon-based instruments like AirCore (Karon et al., 2010). This would allow one to increase the vertical coverage drastically to an almost complete total column (0–30 km) and thus solve the problem of stratospheric uncertainties.

*Acknowledgements.* We would like to thank many people who have contributed to this study:

The members of the IMECC aircraft campaign team: Martin Hertel, Stephan Baum, Huilin Chen, Armin Jordan, Bert Steinberg, Katinka Petersen, Benjamin Sampson, Christof Petri, Ieda Pscheidt, François Truong, Irène Xueref-Remy, Krzysztof Katrynski, Rolf Maser, Harald Franke, Christoph Klaus, Dieter Schell, Svend Engemann.

Debra Wunch from the California Institute of Technology for her calibration data and the detailed information about her analysis.

We acknowledge the support of the European Commission within the 6th Framework Program through the Integrated Infrastructure Initiative IMECC (Infrastructure for Measurement of the European Carbon Cycle), and the Max Planck Society for funding additional flight hours onboard the Lear Jet.

We would also like to thank Julia Marshall from MPI-BGC for helpful comments.

- 20 The service charges for this open access publication have been covered by the Max Planck Society.

## References

- Crisp, D., Atlas, R. M., Breon, F. M., Brown, L. R., Burrows, J. P., Ciais, P., Connor, B. J., Doney, S. C., Fung, I. Y., Jacob, D. J., Miller, C. E., O'Brien, D., Pawson, S., Randerson, J. T., Rayner, P., Salawitch, R. J., Sander, S. P., Sen, B., Stephens, G. L., Tans, P. P., Toon, G. C., Wennberg, P. O., Wofsy, S. C., Yung, Y. L., Kuang, Z., Chudasama, B., Sprague, G., Weiss, B., Pollock, R., Kenyon, D., and Schroll, S.: The Orbiting Carbon Observatory (OCO)

[Title Page](#)

[Abstract](#)

[Introduction](#)

[Conclusions](#)

[References](#)

[Tables](#)

[Figures](#)

◀

▶

◀

▶

[Back](#)

[Close](#)

[Full Screen / Esc](#)

[Printer-friendly Version](#)

[Interactive Discussion](#)



## Calibration of column-averaged CH<sub>4</sub> over European TCCON sites

M. C. Geibel et al.

[Title Page](#)

[Abstract](#)

[Introduction](#)

[Conclusions](#)

[References](#)

[Tables](#)

[Figures](#)



[◀](#)  
[Back](#)

[▶](#)  
[Close](#)

[Full Screen / Esc](#)

[Printer-friendly Version](#)

[Interactive Discussion](#)



- mission, *Adv. Space Res.*, Trace Constituents in the Troposphere and Lower Stratosphere, 34, 700–709, doi:10.1016/j.asr.2003.08.062, 2004. 1519
- Geibel, M. C., Gerbig, C., and Feist, D. G.: A new fully automated FTIR system for total column measurements of greenhouse gases, *Atmos. Meas. Tech.*, 3, 1363–1375, doi:10.5194/amt-3-1363-2010, 2010. 1520
- Gerbig, C., Körner, S., and Lin, J. C.: Vertical mixing in atmospheric tracer transport models: error characterization and propagation, *Atmos. Chem. Phys.*, 8, 591–602, doi:10.5194/acp-8-591-2008, 2008. 1519
- Kalnay, E., Kanamitsu, M., Kistler, R., Collins, W., Deaven, D., Gandin, L., Iredell, M., Saha, S., White, G., Woollen, J., Zhu, Y., Leetmaa, A., Reynolds, R., Chelliah, M., Ebisuzaki, W., Higgins, W., Janowiak, J., Mo, K. C., Ropelewski, C., Wang, J., Jenne, R., and Joseph, D.: The NCEP/NCAR 40-Year Reanalysis Project, *B. Am. Meteorol. Soc.*, 77, 437–471, doi:10.1175/1520-0477(1996)077<0437:TNYRP>2.0.CO;2, 1996. 1524
- Karion, A., Sweeney, C., Tans, P., and Newberger, T.: AirCore: An Innovative Atmospheric Sampling System, *J. Atmos. Ocean. Tech.*, 27, 1839–1853, doi:10.1175/2010JTECHA1448.1, 2010. 1532
- Keppel-Aleks, G., Toon, G. C., Wennberg, P. O., and Deutscher, N. M.: Reducing the impact of source brightness fluctuations on spectra obtained by Fourier-transform spectrometry, *Appl. Opt.*, 46, 4774–4779, doi:10.1364/AO.46.004774, 2007. 1522
- Luo, M., Cicerone, R. J., and Russell III, J. M.: Analysis of Halogen Occultation Experiment HF versus CH<sub>4</sub> correlation plots: Chemistry and transport implications, *J. Geophys. Res.*, 100, 13927–13937, doi:10.1029/95JD00621, 1995. 1524
- Messerschmidt, J., Geibel, M. C., Blumenstock, T., Chen, H., Deutscher, N. M., Engel, A., Feist, D. G., Gerbig, C., Gisi, M., Hase, F., Katrynski, K., Kolle, O., Lavrič, J. V., Notholt, J., Palm, M., Ramonet, M., Rettinger, M., Schmidt, M., Sussmann, R., Toon, G. C., Truong, F., Warneke, T., Wennberg, P. O., Wunch, D., and Xueref-Remy, I.: Calibration of TCCON column-averaged CO<sub>2</sub>: the first aircraft campaign over European TCCON sites, *Atmos. Chem. Phys.*, 11, 10765–10777, doi:10.5194/acp-11-10765-2011, 2011. 1520, 1521, 1522
- Morino, I., Uchino, O., Inoue, M., Yoshida, Y., Yokota, T., Wennberg, P. O., Toon, G. C., Wunch, D., Roehl, C. M., Notholt, J., Warneke, T., Messerschmidt, J., Griffith, D. W. T., Deutscher, N. M., Sherlock, V., Connor, B., Robinson, J., Sussmann, R., and Rettinger, M.: Preliminary validation of column-averaged volume mixing ratios of carbon dioxide and methane retrieved from GOSAT short-wavelength infrared spectra, *Atmos. Meas. Tech.*, 4, 1061–1076,

- Rayner, P. J. and O'Brien, D. M.: The utility of remotely sensed CO<sub>2</sub> concentration data in surface source inversions, *Geophys. Res. Lett.*, 28, 175–178, doi:10.1029/2000GL011912, 2001. 1519
- 5 Rodgers, C. D. and Connor, B. J.: Intercomparison of remote sounding instruments, *J. Geophys. Res.*, 108, 4116–4229, doi:10.1029/2002JD002299, 2003. 1523, 1529
- Washenfelder, R. A., Wennberg, P. O., and Toon, G. C.: Tropospheric methane retrieved from ground-based near-IR solar absorption spectra, *Geophys. Res. Lett.*, 30, 2226, doi:10.1029/2003GL017969, 2003. 1524
- 10 Wunch, D., Toon, G. C., Wennberg, P. O., Wofsy, S. C., Stephens, B. B., Fischer, M. L., Uchino, O., Abshire, J. B., Bernath, P., Biraud, S. C., Blavier, J.-F. L., Boone, C., Bowman, K. P., Browell, E. V., Campos, T., Connor, B. J., Daube, B. C., Deutscher, N. M., Diao, M., Elkins, J. W., Gerbig, C., Gottlieb, E., Griffith, D. W. T., Hurst, D. F., Jiménez, R., Keppel-Aleks, G., Kort, E. A., Macatangay, R., Machida, T., Matsueda, H., Moore, F., Morino, I., Park, S., Robinson, J., Roehl, C. M., Sawa, Y., Sherlock, V., Sweeney, C., Tanaka, T., and Zondlo, M. A.: Calibration of the Total Carbon Column Observing Network using aircraft profile data, *Atmos. Meas. Tech.*, 3, 1351–1362, doi:10.5194/amt-3-1351-2010, 2010. 1518, 1519, 1521, 1523, 1524, 1525, 1526, 1527, 1529, 1530, 1531, 1545, 1548
- 15 Wunch, D., Toon, G. C., Blavier, J.-F. L., Washenfelder, R., Notholt, J., Connor, B. J., Griffith, D. W. T., Sherlock, V., and Wennberg, P. O.: The Total Carbon Column Observing Network (TCCON), *Phil. Trans. R. Soc. A*, 369, 2087–2112, doi:10.1098/rsta.2010.0240, 2011. 1519, 1521
- 20 Yokota, T., Yoshida, Y., Eguchi, N., Ota, Y., Tanaka, T., Watanabe, H., and Maksyutov, S.: Global concentrations of CO<sub>2</sub> and CH<sub>4</sub> retrieved from GOSAT: first preliminary results, *SOLA*, 5, 160–163, doi:10.2151/sola.2009-041, 2009. 1519
- 25 York, D., Evensen, N. M., Martínez, M. L., and Delgado, J. D. B.: Unified equations for the slope, intercept, and standard errors of the best straight line, *Amer. J. Phys.*, 72, 367–375, doi:10.1119/1.1632486, 2004. 1526, 1527

## Calibration of column-averaged CH<sub>4</sub> over European TCCON sites

M. C. Geibel et al.

[Title Page](#)

[Abstract](#)

[Introduction](#)

[Conclusions](#)

[References](#)

[Tables](#)

[Figures](#)

◀

▶

◀

▶

[Back](#)

[Close](#)

[Full Screen / Esc](#)

[Printer-friendly Version](#)

[Interactive Discussion](#)



## Calibration of column-averaged CH<sub>4</sub> over European TCCON sites

M. C. Geibel et al.

[Title Page](#)

[Abstract](#)

[Introduction](#)

[Conclusions](#)

[References](#)

[Tables](#)

[Figures](#)

[◀](#)

[▶](#)

[◀](#)

[▶](#)

[Back](#)

[Close](#)

[Full Screen / Esc](#)

[Printer-friendly Version](#)

[Interactive Discussion](#)

**Table 1.** The sites of the IMECC campaign and their overflight dates.

ID	Location	Latitude	Longitude	Overflights [UTC]	Code
BI	Bialystok, Poland	53.23° N	23.03° E	30 Sep 2009 09:39 10:04 13:48 14:10	BI-OF1a BI-OF1b BI-OF2a BI-OF2b
OR	Orleans, France	47.97° N	2.13° E	10 Feb 2009 06:36 07:02 10:35 10:57	OR-OF1a OR-OF1b OR-OF2a OR-OF2b
KA	Karlsruhe, Germany	49.08° N	8.43° E	10 Feb 2009 09:31	KA-OF1a
GM	Garmisch- Partenkirchen, Germany	47.48° N	11.06° E	10 May 2009 08:47	GM-OF1a
JE	Jena, Germany	50.91° N	11.57° E	10 May 2009 07:56 08:08 10 Sep 2009 10:12 10:35	JE-OF1a JE-OF1b JE-OF2a JE-OF2b
BR	Bremen, Germany	53.10° N	8.85° E	10 May 2009 08:47 10 Sep 2009 11:05	BR-OF1a BR-OF2a

## Calibration of column-averaged CH<sub>4</sub> over European TCCON sites

M. C. Geibel et al.

**Table 2.** Uncertainties related to different parts of the total column that was derived from the aircraft measurements. The main contributions come from the extrapolation to the surface, the aircraft data and the extension of the column to the stratosphere. They are listed as individual uncertainty  $u_p$ , contribution to the total column uncertainty  $u_t$ , and relative contribution to the total aircraft DMF error in %.

Overflight	Mean uncertainties for						Total [ppb]			
	Surface Extrapolation			Aircraft Data						
	$u_p$ [ppb]	$u_t$ [ppb]	[%]	$u_p$ [ppb]	$u_t$ [ppb]	[%]				
BI-OF1a	4.39	0.10	5.35	0.38	0.28	7.51	15.69	3.27	87.14	4.02
BI-OF1b	3.34	0.20	1.81	0.37	0.24	4.32	16.53	5.29	93.87	6.08
BI-OF2a	5.63	0.37	6.16	0.26	0.16	2.63	16.42	5.50	91.21	5.30
BI-OF2b	4.06	0.27	6.29	0.32	0.22	5.15	15.84	3.78	88.56	3.56
BR-OF1a	22.74	1.13	30.62	0.31	0.25	6.72	15.01	2.31	62.65	3.55
BR-OF2a	3.49	0.21	7.67	0.34	0.27	10.02	14.98	2.21	82.32	2.64
GM-OF1a	8.61	0.74	20.46	0.24	0.18	4.93	15.22	2.70	74.61	3.66
JE-OF1a	9.38	0.71	19.32	0.32	0.24	6.52	15.43	2.73	74.16	3.64
JE-OF1b	7.35	0.52	7.74	0.36	0.20	3.03	16.72	5.99	89.23	6.87
JE-OF2a	3.32	0.18	6.18	0.30	0.23	7.86	15.37	2.55	85.96	3.10
JE-OF2b	5.34	0.19	6.30	0.31	0.25	8.31	15.37	2.55	85.40	3.11
KA-OF1a	7.51	0.46	0.51	0.46	0.27	3.59	17.14	7.15	95.91	7.49
OR-OF1a	7.06	0.08	11.70	0.41	0.30	7.69	15.42	3.61	80.61	2.69
OR-OF1b	1.08	0.18	1.19	0.40	0.21	3.10	16.50	6.25	95.70	5.09
OR-OF2b	3.86	0.04	3.99	0.48	0.29	4.55	16.67	5.75	91.46	6.88
average	6.26	0.35	8.75	0.36	0.24	5.88	15.89	4.05	85.38	4.50

[Title Page](#)[Abstract](#)[Introduction](#)[Conclusions](#)[References](#)[Tables](#)[Figures](#)[◀](#)[▶](#)[◀](#)[▶](#)[Back](#)[Close](#)[Full Screen / Esc](#)[Printer-friendly Version](#)[Interactive Discussion](#)

## Calibration of column-averaged CH<sub>4</sub> over European TCCON sites

M. C. Geibel et al.

**Table 3.** Results of the IMECC campaign.

Calibration factor	A-priori profile	Dataset	Value	Fit error ( $\pm 1\sigma$ )	Species uncertainty ( $\pm 2\sigma$ )
$\psi_{\text{std}}$	standard GFIT	IMECC	0.978	$\pm 0.0021$	$\pm 7 \text{ ppb}$
$\psi_{\text{aircraft}}$	ext. aircraft	IMECC	0.978	$\pm 0.0021$	$\pm 7 \text{ ppb}$
$\psi_{1+W}$	ext. aircraft	IMECC + Wunch et al.	0.978	$\pm 0.0007$	$\pm 2.3 \text{ ppb}$
$\psi_n$	ext. aircraft	IMECC	0.974	$\pm 0.0020$	$\pm 7 \text{ ppb}$
WMO recommendation for in-situ measurements				$\pm 2 \text{ ppb}$	

- [Title Page](#)
- [Abstract](#) [Introduction](#)
- [Conclusions](#) [References](#)
- [Tables](#) [Figures](#)
- [◀](#) [▶](#)
- [◀](#) [▶](#)
- [Back](#) [Close](#)
- [Full Screen / Esc](#)
- [Printer-friendly Version](#)
- [Interactive Discussion](#)



**Fig. 1.** FTS locations and aircraft flight tracks of the IMECC campaign. The aircraft was stationed at a military airbase near Hohn in northern Germany.

## Calibration of column-averaged CH<sub>4</sub> over European TCCON sites

M. C. Geibel et al.

[Title Page](#)

[Abstract](#)

[Introduction](#)

[Conclusions](#)

[References](#)

[Tables](#)

[Figures](#)

◀

▶

◀

▶

[Back](#)

[Close](#)

[Full Screen / Esc](#)

[Printer-friendly Version](#)

[Interactive Discussion](#)

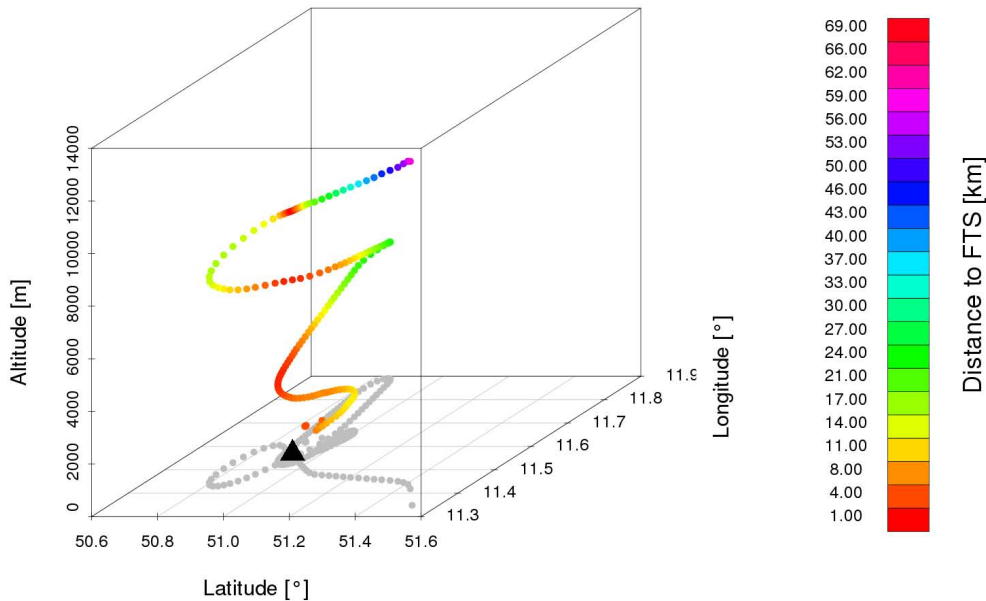


**Fig. 2.** A typical aircraft profile with spiral close to the FTS location. This figure shows the overflight JE-OF2a. The black triangle symbolizes the location of the FTS. The colors of the dots symbolize the distance of the aircraft to the FTS, the grey dots are a projection of the flight path on the ground. The corresponding aircraft data are shown in Fig. 3.

## Calibration of column-averaged CH<sub>4</sub> over European TCCON sites

M. C. Geibel et al.

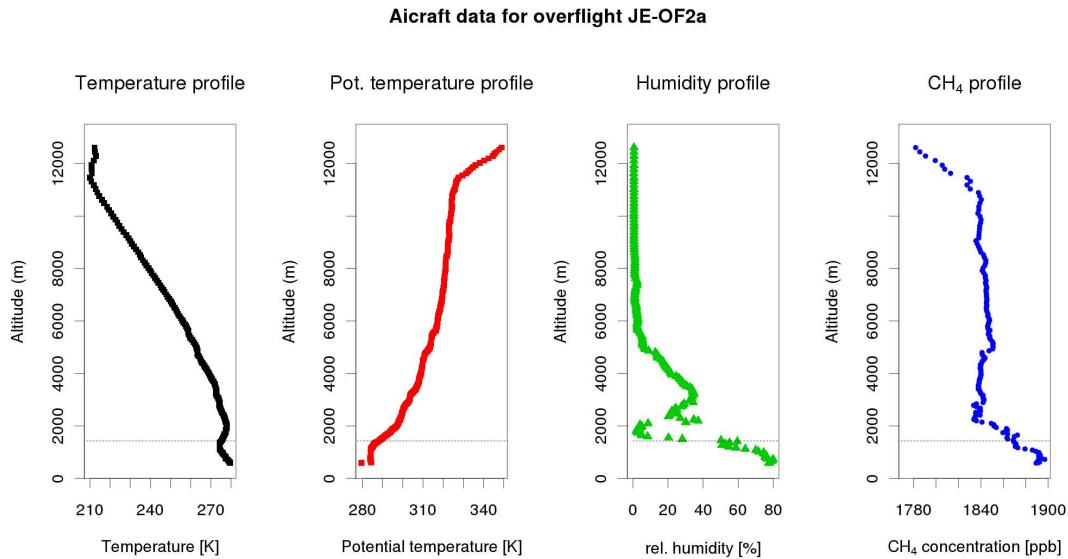


**Fig. 3.** CH<sub>4</sub>, H<sub>2</sub>O and temperature data from aircraft in-situ measurements obtained during the overflight JE-OF2a. The potential temperature was calculated from the temperature and pressure profile. The dashed line illustrates the calculated boundary layer height. At the time of the overflight the boundary layer height at Jena was approximately 1700 m.

[Title Page](#)

[Abstract](#)

[Introduction](#)

[Conclusions](#)

[References](#)

[Tables](#)

[Figures](#)

◀

▶

◀

▶

[Back](#)

[Close](#)

[Full Screen / Esc](#)

[Printer-friendly Version](#)

[Interactive Discussion](#)

# Calibration of column-averaged CH<sub>4</sub> over European TCCON sites

M. C. Geibel et al.

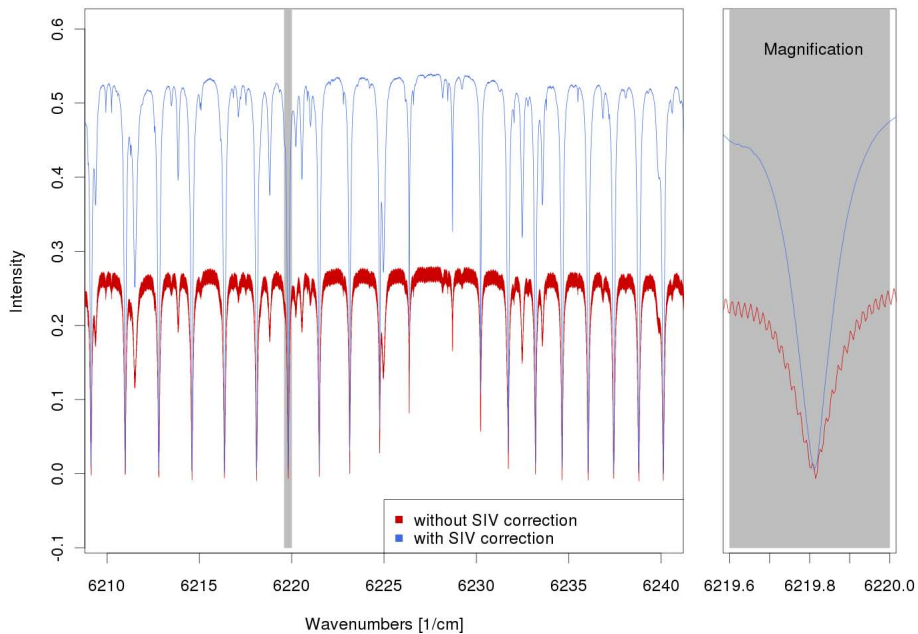


**Fig. 4.** Influence of the correction of the solar intensity variations (SIV) performed with opus-ipp software on the noise level of the spectrum. In the magnification the resulting spectrum shows a significantly increased signal to noise ratio.

Title Page

## Abstract

Abstract Introduction

## Conclusion

## Inclusions References

Tables

Tables | Figures



Back

[Close](#)

Full Screen / Esc

[Printer-friendly Version](#)

Interactive Discussion

## Calibration of column-averaged CH<sub>4</sub> over European TCCON sites

M. C. Geibel et al.

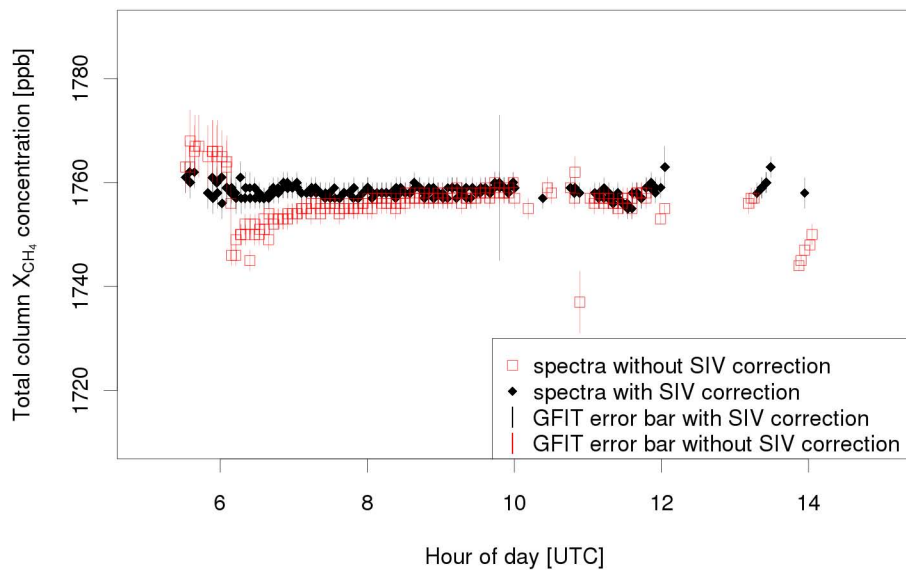


**Fig. 5.** Influence of the SIV correction performed with the IPP software (in this case slice\_ipp) on the GFIT retrieval on the IMECC flight campaign FTS data of Bialystok.

- [Title Page](#)
- [Abstract](#) [Introduction](#)
- [Conclusions](#) [References](#)
- [Tables](#) [Figures](#)
- [◀](#) [▶](#)
- [◀](#) [▶](#)
- [Back](#) [Close](#)
- [Full Screen / Esc](#)
- [Printer-friendly Version](#)
- [Interactive Discussion](#)

## Calibration of column-averaged $\text{CH}_4$ over European TCCON sites

M. C. Geibel et al.

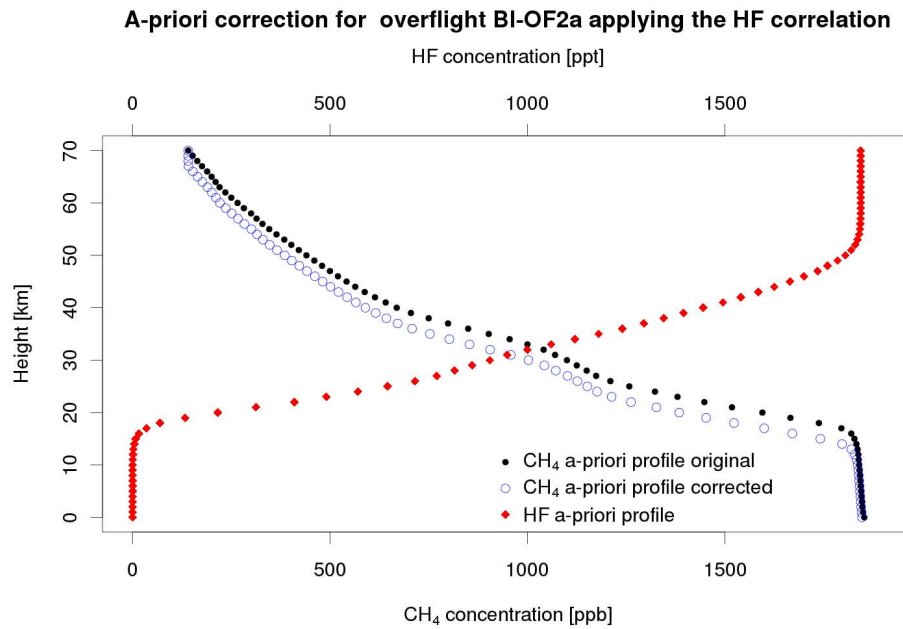


**Fig. 6.** The effect of applying the  $\text{CH}_4$ -HF-correlation to the  $\text{CH}_4$  GFIT a-priori profile shown for the example of the overflight BI-OF2a.

- [Title Page](#)
- [Abstract](#) [Introduction](#)
- [Conclusions](#) [References](#)
- [Tables](#) [Figures](#)
- [◀](#) [▶](#)
- [◀](#) [▶](#)
- [Back](#) [Close](#)
- [Full Screen / Esc](#)
- [Printer-friendly Version](#)
- [Interactive Discussion](#)

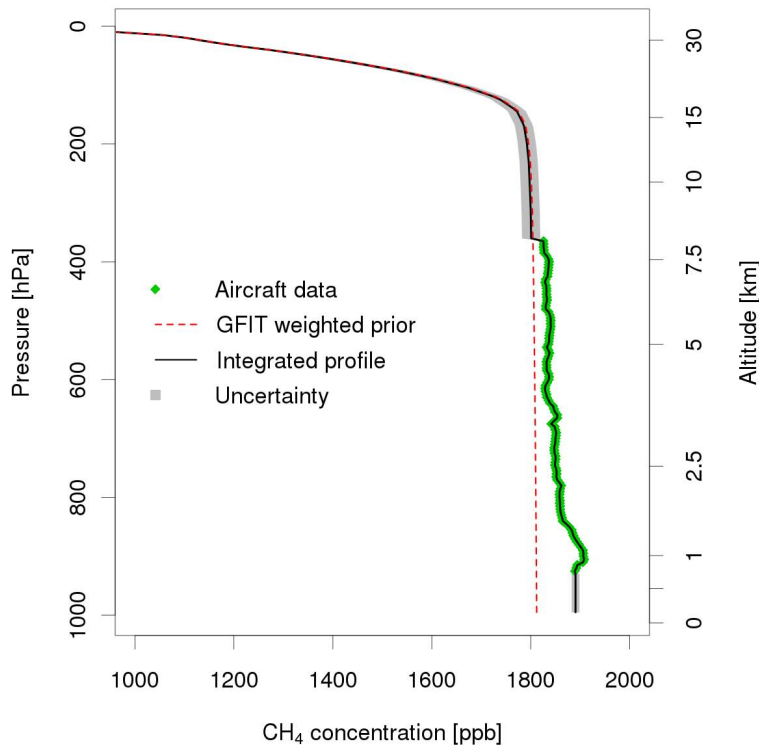


**Fig. 7.** Example for the extension of aircraft data to a total column (JE-OF1b). The green partial column represents the aircraft in-situ data. This column was extended by the weighted GFIT a-priori in the stratosphere. The lower part was extended to the ground by adding ground-based in-situ data where available. Otherwise the profile was extrapolated to the surface. The gray area represents the uncertainty of the extended parts. The red line represents the weighted GFIT a-priori profile.

## Calibration of column-averaged $\text{CH}_4$ over European TCCON sites

M. C. Geibel et al.

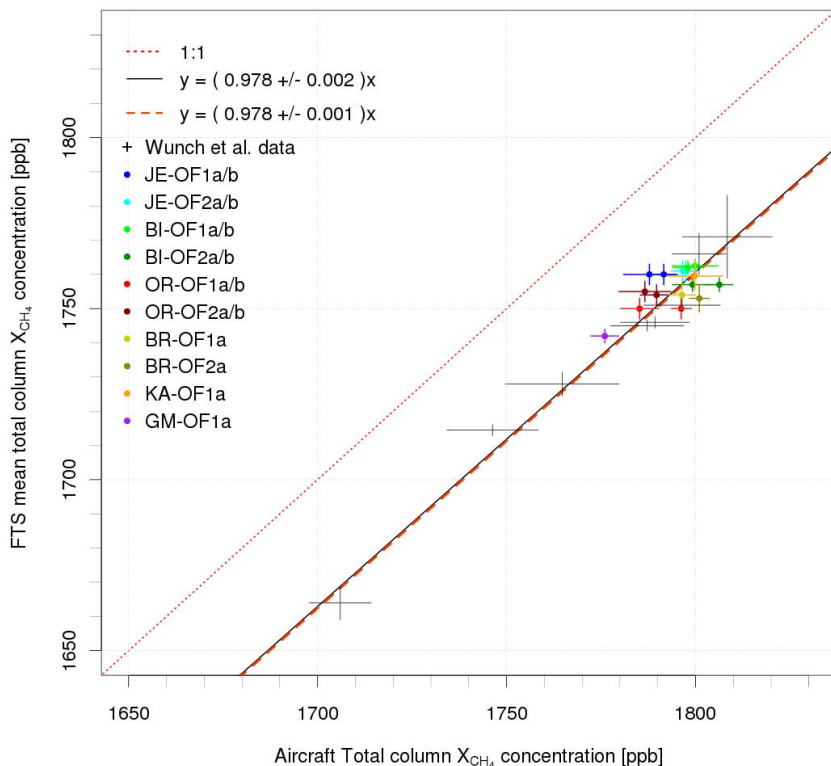


**Fig. 8.** Calibration factor of  $\text{CH}_4$  for all data including Wunch et al. (2010) data derived from the GFIT retrieval with aircraft profiles as a-priori. The black continuous line represents the fit for calibration factor  $\psi_{\text{aircraft}}$  derived for the IMECC data. The dark-orange dashed line represents the fit for calibration factor  $\psi_{+w}$  for all sites (IMECC + Wunch et al.). Both fits are nearly identical.

1545

## Calibration of column-averaged $\text{CH}_4$ over European TCCON sites

M. C. Geibel et al.

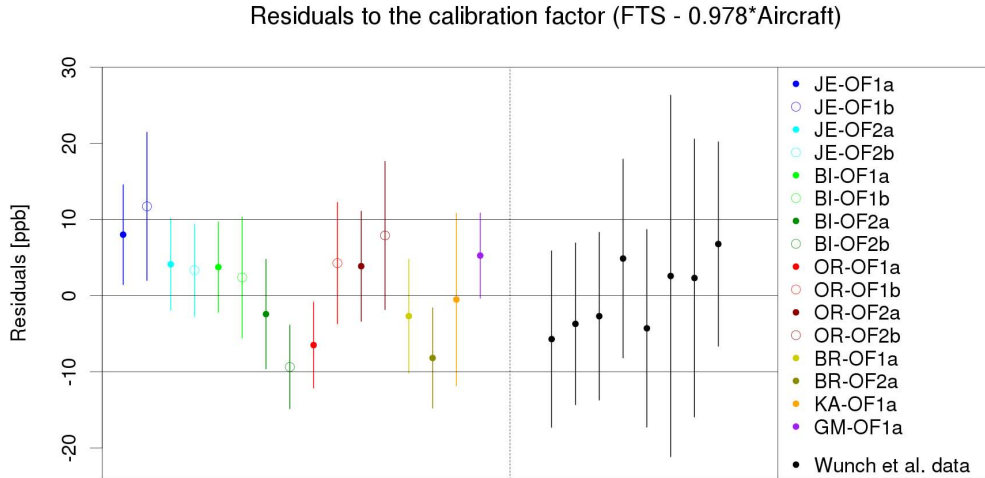


**Fig. 9.** Residuals ( $\text{DMF}_{\text{FTS}} - \psi_{l+w} \text{DMF}_{\text{aircraft}}$ ) calculated for all calibration points using aircraft profiles as a-priori for the GFIT retrieval. The error bars are the squared sum of the FTS and the aircraft errors.

1546

## Calibration of column-averaged $\text{CH}_4$ over European TCCON sites

M. C. Geibel et al.

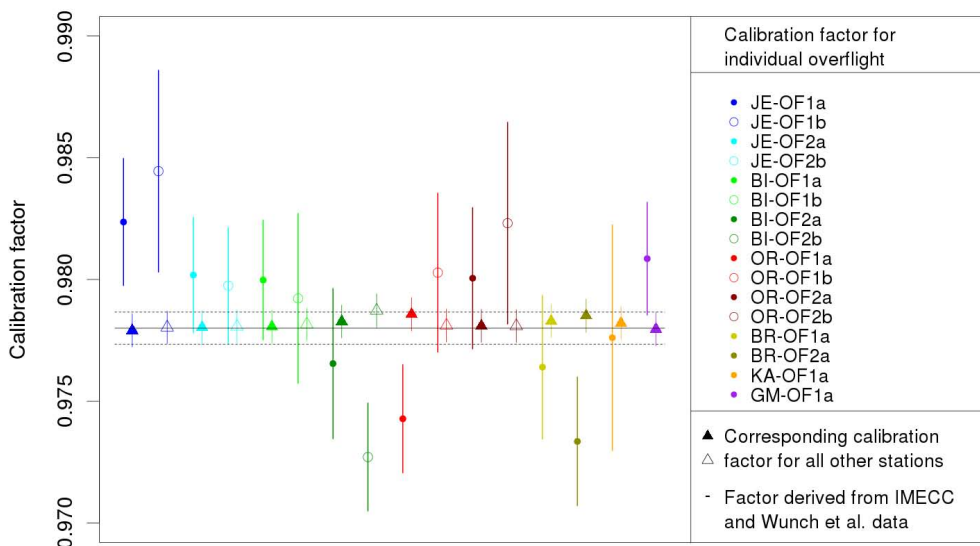


**Fig. 10.** Influence of the individual overflights of the IMECC sites on the calibration factor. For this study, the calibration factor for each individual overflight and the artificial calibration point in the origin were derived (full and empty dots). An additional calibration factor was calculated for the corresponding remaining overflights and the artificial calibration point in the origin (full and empty triangles). The error bars of the overflights JE-OF1a, JE-OF1b, BI-OF2b, OR-OF1a and BR-OF2a do not overlap with the respective calibration factors derived from the overflights over the corresponding remaining sites.

## Calibration of column-averaged CH<sub>4</sub> over European TCCON sites

M. C. Geibel et al.

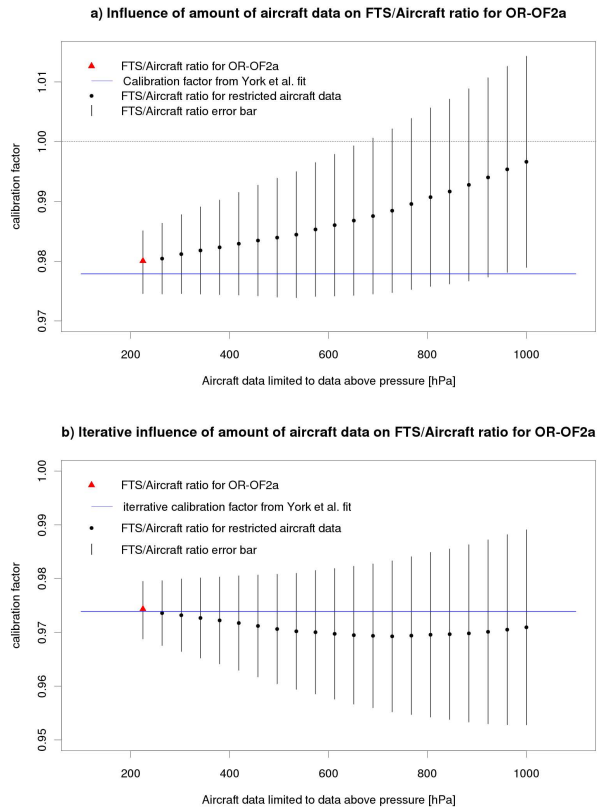


**Fig. 11.** (a) Influence of the vertical coverage of aircraft data in the aircraft column on the derived FTS-to-aircraft ratio illustrated for the example of OR-OF2a. The red triangle symbolizes the FTS-to-aircraft ratio for this overflight. The blue line is the calibration factor determined for all sites (incl. Wunch et al. (2010) data). The black dots symbolize the FTS-to-aircraft ratio calculated with a restricted vertical coverage of aircraft data in the aircraft column. The fewer aircraft data available, the more the calibration factor converges to 1. The error bars are a combination of FTS and aircraft error and increased with decreasing vertical coverage. (b) Influence of the vertical coverage of aircraft data in the aircraft column on the derived FTS-to-aircraft ratio for the iterative approach illustrated on the example of OR-OF2a. The amount of aircraft data does no longer show an significant influence on the calibration factor.

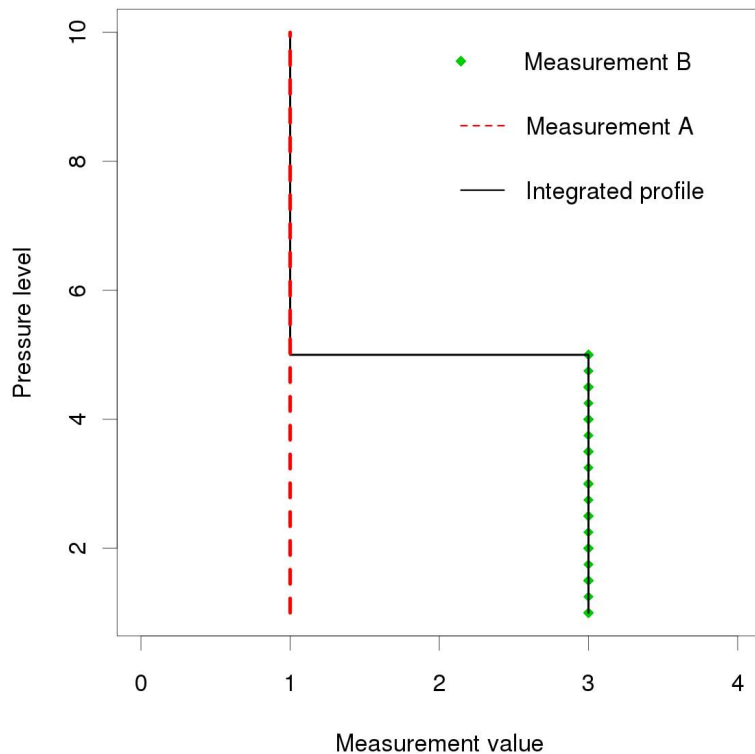


**Fig. 12.** Illustration of the bias introduced by the extrapolation of measurement B to a total column using data of measurement A. The integrated profile leads to a calibration value of 2, while the true value should be 3.

**Fig. 13.** Example for the extension of aircraft data to a total column (JE-OF1b) using an a-priori profile scaled with an iteratively-derived calibration factor (blue).

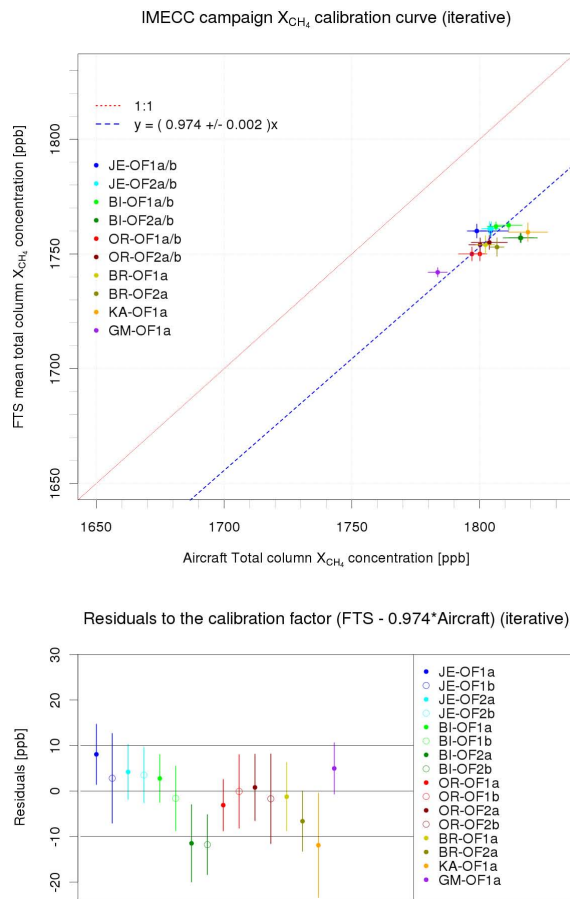


**Fig. 14.** Upper part: calibration factor derived by an iterative calculation for the IMECC campaign data. Lower part: corresponding residuals.